Articles

Contribution from the Laboratoire de Chimie et Biochimie Pharmacologiques et Toxicologiques, Université René Descartes, 75270 Paris Cedex 06, France, and Laboratoire de Physicochimie Inorganique, Université Pierre et Marie Curie, 75230 Paris Cedex 05, France

Sequence-Dependent Platinum Chelation by Adenylyl(3′–5′)guanosine and Guanylyl(3′–5′)adenosine Reacting with *cis*-Diamminedichloroplatinum(II) and Its Diaqua Derivative[1]

Bruno Van Hemelryck,[2a] Jean-Pierre Girault,[2a] Genevieve Chottard,[2b] Philippe Valadon,[2a,c] Abdelazize Laoui,[2a] and Jean-Claude Chottard*[2a]

Received July 29, 1986

Ribo-ApG and ribo-GpA react with *cis*-$[PtCl_2(NH_3)_2]$ or *cis*-$[Pt(NH_3)_2(H_2O)_2](NO_3)_2$ (one Pt per dinucleotide, ca. 10^{-4} M in water at pH 5.5) to give various types of platinum chelates. The dichloro and diaqua species lead to the same product distributions. The adducts formed have been characterized by atomic absorption spectroscopy, high-pressure gel-permeation chromatography, high-field ^1H NMR (by studies of the pH dependence of the nonexchangeable base proton signals, of the purine H8–deuterium exchange rates, of T_1 relaxation times and of nuclear Overhauser effects) and by circular dichroism. ApG gives a single AN7-GN7 chelate (>95%), *cis*-$[Pt(NH_3)_2(ApG\text{-}N7(1),N7(2))]^+$ (**1**), with an anti,anti configuration of the bases. **1** is in every respect similar to the previously described GpG·*cis*-Pt chelate. GpA gives four isomeric platinum adducts, one GN7-AN1 chelate **2** (32% of the mixture) and three GN7-AN7 chelates **3** (5%), **4** (42%), and **5** (21%). *cis*-$[Pt(NH_3)_2(GpA\text{-}N7(1),N1(2))]^+$ (**2**) presents a relatively fast rotation of the adenine about its glycosidic and N1–Pt bonds (k_1 = 1.4 (2) s^{-1} for the conversion of the major into the minor conformer at 18 °C, K_{291} = 0.54). The *cis*-$[Pt(NH_3)_2(GpA\text{-}N7(1),N7(2))]^+$ isomers **4** and **5** are respectively $G_{anti}A_{anti}$ and $G_{anti}A_{syn}$. A $G_{syn}A_{syn}$ structure is tentatively assigned to complex **3**. ApG and GpA react with *cis*-$[Pt(NH_3)_2(H_2O)_2](NO_3)_2$ to first give a GN7 monocoordinated intermediate complex characterized as *cis*-$[Pt(NH_3)_2(H_2O)(ApG\text{-}N7(2))]^+$ (**8**) in the case of ApG. Kinetic studies, based on UV and HPLC monitoring of the reactions, have shown that, for the first platination step, ApG reacts 2 times faster than GpA (k_1 = 1.7 (1) and 0.8 (1) $M^{-1}\cdot s^{-1}$, respectively) whereas the chelation step of the ApG intermediate is 3 times slower than that of the GpA one (k_2 = 1.5 (1) × 10^{-4} and 4.5 (2) × 10^{-4} s^{-1}, respectively). These results are attributed for the first step to charge interaction and/or hydrogen bonding between the cationic aquated platinum species and the monoanionic phosphodiester group, favoring N7 platination of the 3′-purine, and for the chelation step to hydrogen bonding, within the intermediate complex **8**, between the phosphodiester bridge and an ammine or aqua ligand of platinum. The latter interaction prevents G rotation and favors base stacking, leading to formation of the single AN7-GN7 anti,anti chelate.

DNA is the primary cellular target of the aquated forms[3] of the antitumor drug *cis*-$PtCl_2(NH_3)_2$[4,5] (*cis*-DDP).[6] Studies with various DNAs have shown that intrastrand cross-linking of two adjacent guanines is the major coordination fate (40–60%) of the *cis*-$Pt(NH_3)_2^{2+}$ moiety,[7-10] followed by cross-linking of the d(ApG) sequence (ca. 20%).[9,10] An X-ray structure analysis, at 6-Å resolution, of platinated tRNAPhe also pointed to the presence of the GpG and ApG platinum chelates together with the CpG one.[11] Other less frequent types of chelation have been proposed, from the analysis of enzymatic digests of platinated DNA, that involve either the two guanines or the adenine and guanine of the d(GpXpG)[9,10] and d(ApXpG)[10] sequences with X = A, C, T. Model studies with dinucleotides[12,13] and with larger oligonucleotides[14-20] all concluded that platinum chelation by two

(1) Presented in part at the Second International Conference on Bioinorganic Chemistry, Algarve, Portugal, April 1985.
(2) (a) Université René Descartes, Unité Associée au CNRS en développement concerté avec l'INSERM (UA 400). (b) Université Pierre et Marie Curie, Unité Associée au CNRS (UA 419). (c) 4th-year medical student at Centre Hospitalo-Universitaire Necker-Enfants malades.
(3) Martin, R. B. In *Platinum, Gold and Other Metal Chemotherapeutic Agents*; Lippard, S. J., Ed.; ACS Symposium Series 209; American Chemical Society: Washington, DC, 1983; pp 231–244.
(4) Roberts, J. J.; Thomson, A. J. *Prog. Nucleic Acid Res. Mol. Biol.* **1979**, *22*, 71–133.
(5) Pinto, A. L.; Lippard, S. J. *Biochim. Biophys. Acta* **1985**, *780*, 167–180.
(6) (a) Abbreviations: *cis*-DDP, *cis*-diamminedichloroplatinum(II); dien, diethylenetriamine; TSP-d_4, sodium 3-(trimethylsilyl)-1-propionate-2,2,3,3-d_4; HPLC, high-pressure liquid chromatography; NOE, nuclear Overhauser effect. A and G represent adenosine and guanosine; d = deoxy. The letter p to the left of a nucleoside symbol indicates a 5′-phosphate and to the right indicates a 3′-phosphate. (b) The common nomenclature for inorganic compounds is combined with that recommended by the IUPAC-IUB for nucleic acids (*Eur. J. Biochem.* **1983**, *131*, 9–15). In formulas the coordinating atoms of the oligonucleotide are indicated after the ligand, separated by a hyphen and set in italics, e.g. *cis*-$[Pt(NH_3)_2(GpA\text{-}N7(1),N1(2))]^+$. *cis*-Pt is used for the *cis*-$Pt(NH_3)_2^{2+}$ moiety. The following abbreviations are also used for the complexes, e.g.: *cis*-$[Pt(NH_3)_2(ApG\text{-}N7(1),N7(2))]^+$ (**1**) = ApG·*cis*-Pt (**1**); $[Pt(dien)(ApG\text{-}N7(2))]^+$ (**6**) = ApG·Pt(dien) (**6**).
(7) Kelman, A. D.; Buchbinder, M. *Biochimie* **1978**, *60*, 893–899.
(8) (a) Cohen, G. L.; Ledner, J. A.; Bauer, W. R.; Ushay, H. M.; Caravana, C.; Lippard, S. J. *J. Am. Chem. Soc.* **1980**, *102*, 2487–2488. (b) Ushay, H. M.; Tullius, T. D.; Lippard, S. J. *Biochemistry* **1981**, *20*, 3744–3748. (c) Tullis, T. D.; Lippard, S. J. *J. Am Chem. Soc.* **1981**, *103*, 4620–4622.
(9) (a) Fichtinger-Schepman, A.-M. J.; Lohman, P. H. M.; Reedijk, J. *Nucleic Acids Res.* **1982**, *10*, 5345–5356. (b) Fichtinger-Schepman, A.-M. J.; Van der Veer, J. L.; den Hartog, J. H. J.; Lohman, P. H. M.; Reedijk, J. *Biochemistry* **1985**, *24*, 707–713. (c) Plooy, A. C. M.; Fichtinger-Schepman, A.-M. J.; Schutte, H. H.; van Dijk, M.; Lohman, P. H. M. *Carcinogenesis (London)* **1985**, *6*, 561–566.
(10) Eastman, A. *Biochemistry* **1983**, *22*, 3927–3933.
(11) Dewan, J. C. *J. Am. Chem. Soc.* **1984**, *106*, 7239–7244.
(12) (a) Chottard, J.-C.; Girault, J.-P.; Chottard, G.; Lallemand, J. Y.; Mansuy, D. *J. Am. Chem. Soc.* **1980**, *102*, 5565–5572. (b) Girault, J.-P.; Chottard, G.; Lallemand, J. Y.; Chottard, J.-C. *Biochemistry* **1982**, *21*, 1352–1356.
(13) Inagaki, K.; Kasuya, K.; Kidani, Y. *Chem. Lett.* **1983**, 1345–1348.
(14) (a) Marcelis, A. T. M.; Canters, G. W.; Reedijk, J. *Recl. Trav. Chim. Pays-Bas* **1981**, *100*, 391–392. (b) Marcelis, A. T. M.; den Hartog, J. H. J.; van den Marel, G. A.; Wille, G.; Reedijk, J. *Eur. J. Biochem.* **1983**, *135*, 343–349.
(15) Inagaki, K.; Kasuya, K.; Kidani, Y. *Inorg. Chim. Acta* **1984**, *91*, L13–L15.
(16) Caradonna. J. P.; Lippard, S. J.; Gait, M. J.; Singh, M. *J. Am. Chem. Soc.* **1982**, *104*, 5793–5795.
(17) (a) Girault, J.-P.; Chottard, J.-C.; Guittet, E. R.; Lallemand, J. Y.; Huynh-Dinh, T.; Igolen, J. *Biochem. Biophys. Res. Commun.* **1982**, *109*, 1157–1163. (b) Chottard, J.-C.; Girault, J.-P.; Guittet, E.; Lallemand, J. Y.; Huynh-Dinh, T.; Igolen, J.; Neumann, J.; Tran-Dinh, S. *Inorg. Chim. Acta* **1983**, *79*(B7), 249–250.

0020-1669/87/1326-0787$01.50/0

adjacent guanines is a kinetically favored pathway, giving a single GN7-GN7 anti,anti complex.[21-23] Model chelations by the GCG sequence have also been described.[24,25] Considering the structural analogy between the AG and GA sequences, the absence of a d(GpA) chelate in the digests of platinated DNA[9,10] asks for comparative data for the first GN7 platination step and for the chelation step of the two sequences. Dinucleotide studies have already revealed a striking difference between platinum chelation by the GC and CG sequences. While CpG and d(pCpG) give only one CN3-GN7 chelate (with G anti and C flipping between the syn and anti conformations),[26] GpC and d(pGpC) give the two couples of GN7-CN3 isomers (with G anti and G syn).[27] The present paper reports a comparative study of the reactions of ribo-ApG and GpA with *cis*-DDP and its diaqua derivative. It shows that ApG behaves like GpG and gives only the AN7-GN7 anti,anti platinum chelate. GpA gives a mixture of four isomers: a GN7-AN1 chelate and three GN7-AN7 chelates. Adenine rotation is demonstrated for the GN7-AN1 isomer. During the course of this work, a UV spectral analysis of the reaction mixture of GpA with *cis*-DDP concluded to the presence of two products. One was shown to be a GN7-AN7 chelate, but no definite assignment was proposed for the other.[28] For ApG and GpA reacting with the *cis*-$[Pt(NH_3)_2(H_2O)_2]^{2+}$ complex, the rates of GN7 platination and of the second step chelation are compared.

Experimental Section

rApG and rGpA ammonium salts were from Sigma. The stoichiometric reactions (one Pt per dinucleotide) were run at 10^{-4} to 4×10^{-4} M concentrations at pH ca. 5.5, in doubly distilled water, at 37 °C with *cis*-DDP, its diaqua derivative, or [PtCl(dien)]Cl, under previously described conditions.[12,26,27] The predominant reactive species are the aqua chloro and aqua hydroxo complexes for *cis*-DDP and the diaqua and aqua hydroxo complexes for *cis*-$[Pt(NH_3)_2(H_2O)_2](NO_3)_2$.[3]

The platinum content of the complexes was determined by atomic absorption using a Perkin-Elmer A 560 spectrometer coupled with an HGA 500 programmator.

HPLC analyses and preparative separations were performed on Altex 420 and Beckman 421 liquid chromatographs, with 254-nm detection, on Waters C_{18} Micro-Bondapak and Bishop Nucleosil 100 columns used in reverse phase. Two elution systems were used: 10^{-2} M aqueous $CH_3CO_2NH_4$, pH 4.7 (A_1), and 10^{-2} M $CH_3CO_2NH_4$ in H_2O/CH_3OH (1:1), pH 4.7 (B_1) (15–60% gradient); 10^{-2} M aqueous $CH_3CO_2((C_2H_5)_3NH)$, pH 6.5 (A_2), and H_2O/CH_3CN (1:1) (B_2) (5–20% gradient). We have not been able to resolve the second fraction of the GpA reaction mixture also with RP 300, DEAE (anion exchange), and Serva (diethylamino)ethyl columns.

High-pressure gel-permeation chromatography analyses were performed on a Waters Micro-Porasil GPC 60-A column using a 0.5 M $CH_3CO_2NH_4$ solution at pH 4 (CH_3CO_2H added) with 1% sodium dodecyl sulfate as eluent.

The ^1H NMR spectra were recorded on Bruker WM 250 (250 MHz) and WM 400 (400 MHz) spectrometers, with use of standard Fourier transform techniques. TSP-d_4 was used as internal standard. The proton T_1 relaxation times were obtained by the inversion recovery method at ca. 20 °C in previously reported conditions.[12b] The analyses of the spectra were obtained by homodecoupling techniques, NOE difference experiments, and two-dimensional homonuclear experiments (2D COSY 45[29] or 2D NOESY;[30] the original data set of 1024 points in the t_2 dimension and 256 points in the t_1 dimension; the resulting data matrix processed with a sine-bell window in the two dimensions and a zero-filling in the f_1 dimension; absolute value mode used). For the magnetization transfer experiments with the A-H8 of the GpA·*cis*-Pt complex **2** all the recording conditions were the same as in the T_1 experiments, except that the selective 180° pulse was obtained by the DANTE pulse sequence.[31] The time necessary for these experiments, about 10 h, was sufficiently short compared to the time of A-H8 deuterium exchange.

The CD spectra were recorded on a Jobin Yvon Mark III instrument. The $\Delta\epsilon$ values ($\epsilon_L - \epsilon_R$, $M^{-1}\cdot cm^{-1}$) are given per nucleotide residue. The molar extinction coefficients of the complexes were determined from the ratio of the optical densities of the dinucleotide solution before and after reaction with the platinum complex, assuming that no concentration change had occurred. For the mixture of the GpA·*cis*-Pt isomers, a mean extinction coefficient was obtained that was used for each isomer separated by HPLC.

For kinetic studies, the UV absorbance or HPLC integration data were analyzed by nonlinear regression by the Marquardt algorithm,[43] with a Minc Digital PDP 11/23 computer, as previously described.[44]

Results

Analysis of the Reactions. ApG and GpA react with 1 molar equiv of *cis*-$[PtCl_2(NH_3)_2]$ ($(1-3) \times 10^{-4}$ M) or of *cis*-$[Pt(NH_3)_2(H_2O)_2](NO_3)_2$ ($(1.7-4) \times 10^{-4}$ M), in water at pH 5.5, to give a solution with a bathochromic shift (λ_{max} at 263 nm compared to 256.5 and 257.5 nm for the ApG an GpA initial solutions). In each case the ratio of the optical densities after and before platination is 0.93 (2). With the *cis*-diaqua complex HPLC shows that ApG and GpA (ca. 2×10^{-4} M) are completely converted into the final adducts after about 18 h. This requires about 35 h with *cis*-DDP.

A comparable evolution is observed for the stoichiometric reaction of ApG and GpA (10^{-4} M) with [PtCl(dien)]Cl (dinucleotide, dinucleotide λ_{max}, Pt adduct λ_{max}, ratio of Pt adduct and dinucleotide optical densities): ApG, 256.5 nm, 257 nm, 0.98 (2); GpA, 257.5 nm, 260 nm, 0.95 (2).

In our concentration range, ApG reacts with the *cis*-diaqua or dichloro complex to give a very predominant adduct (more than 95% from HPLC and ^1H NMR), later called complex **1**. Under the same conditions, GpA gives a mixture of adducts that can be separated by preparative HPLC into two fractions. The first fraction (32% of the mixture from UV and ^1H NMR) corresponds to one adduct:complex **2**. We have not been able to resolve the overlapping peaks of the second fraction. It contains three complexes, later called **3–5**, which represent respectively 5, 42, and 21% (from ^1H NMR) of the overall GpA adduct mixture. With [PtCl(dien)]Cl, ApG and GpA give the single complexes **6** and **7**, respectively.

Analysis of the Complexes Formed. Atomic absorption spectroscopy, together with the UV absorption of the platinum adducts, allowed the determination of the following molar extinction coefficients per platinum (ϵ_{max}/Pt, M^{-1} cm^{-1}): ApG·*cis*-Pt (**1**), 18 300; GpA·*cis*-Pt (**2**), 19 100; GpA·*cis*-Pt (**3** + **4** + **5**), mean ϵ_{max}/Pt 21 800. Compared to an estimated extinction coefficient of 18 000 for the free dinucleotides, this suggests that all the complexes formed contain one platinum per dinucleotide.

Gel-permeation chromatography shows that the retention times of the platinum adducts **1–5** are similar to those of the monodentate complexes **6** and **7** (vide infra) and to that of the previously described GpG·*cis*-Pt N7,N7 chelate.[12b] This indicates that the platinum adducts are monomeric.

ApG Complexes: *cis*-$[Pt(NH_3)_2$(ApG-*N7*(1),*N7*(2))$]^+$ (1) and $[Pt$(dien)(ApG-*N7*(2))$]^+$ (6). Table I gives the ^1H NMR data

(18) (a) den Hartog, J. H. J.; Altona, C.; van Boom, J. H.; van der Marel, G. A.; Haasnoot, C. A. G.; Reedijk, J. *J. Am. Chem. Soc.* **1984**, *106*, 1528–1530. (b) den Hartog, J. H. J.; Altona, C.; van Boom, J. H.; van der Marel, G. A.; Haasnoot, C. A. G.; Reedijk, J. *J. Biomol. Struct. and Dynamics*, **1985**, *2*, 1137–1155.
(19) Van Hemelryck, B.; Guittet, E.; Chottard, G.; Girault, J.-P.; Huynh-Dinh, T.; Lallemand, J. Y.; Igolen, J.; Chottard, J.-C. *J. Am. Chem. Soc.* **1984**, *106*, 3037–3039.
(20) Inagaki, K.; Kidani, Y. *Inorg. Chim. Acta* **1985**, *106*, 187–191.
(21) den Hartog, J. H. J.; Altona, C.; Chottard, J.-C.; Girault, J.-P.; Lallemand, J. Y.; de Leeuw, F. A. A. M.; Marcelis, A. T. M.; Reedijk, J. *Nucleic Acids Res.* **1982**, *10*, 4715–4730.
(22) Neumann, J. M.; Tran-Dinh, S.; Girault, J.-P.; Chottard, J.-C.; Huynh-Dinh, T.; Igolen, J. *Eur. J. Biochem.* **1984**, *141*, 465–472.
(23) Sherman, S. E.; Gibson, D.; Wang, A. H. J.; Lippard, S. J. *Science (Washington, D.C.)* **1985**, *230*, 412–417.
(24) den Hartog, J. H. J.; Altona, C.; van Boom, J. H.; Marcelis, A. T. M.; van den Marel, G. A.; Rinkel, L. J.; Willie Hazeleger, C.; Reedijk, J. *Eur. J. Biochem.* **1983**, *134*, 485–495.
(25) Inagaki, K.; Kidani, Y. *Norg. Chim. Acta* **1984**, *92*, L9–L11.
(26) Girault, J.-P.; Chottard, G.; Lallemand, J. Y.; Huguenin, F.; Chottard, J.-C. *J. Am. Chem. Soc.* **1984**, *106*, 7227–7232.
(27) Chottard, J.-C.; Girault, J.-P.; Guittet, E. R.; Lallemand, J. Y.; Chottard, G. In *Platinum, Gold and Other Metal Chemotherapeutic Agents*; Lippard, S. J., Ed.; ACS Symposium Series 209; American Chemical Society: Washington, DC, 1983; pp 125–145.
(28) Inagaki, K.; Kidani, Y. *Inorg. Chim. Acta* **1983**, *80*, 171–176.
(29) Bax, A.; Freeman, R. *J. Magn. Reson.* **1981**, *44*, 542–561.
(30) Macura, S.; Ernst, R. R. *Mol. Phys.* **1980**, *41*, 95–117.
(31) Moris, G. A.; Freeman, R. *J. Magn. Reson.* **1978**, *29*, 433–462.

Table I. ^{1}H NMR Data for the ApG Complexes: *cis*-[Pt(NH$_3$)$_2$(ApG-*N*7(1),*N*7(2))]$^+$ (**1**) and [Pt(dien)(ApG-*N*7(2))]$^+$ (**6**)[a]

	ApG (pH* 7)		ApG·*cis*-Pt (**1**) (pH* 6.5)[b]			ApG·Pt(dien) (**6**) (pH* 57)		
	δ	J, Hz[c]	δ	J, Hz[c]	$\Delta\delta$[d]	δ	J, Hz[c]	$\Delta\delta$[d]
A-H8	8.22	s	9.26	s	1.04	8.52	s	0.3
G-H8	7.91	s	8.45	s	0.54	8.18	s	0.27
A-H2	8.06	s	8.28	s	0.22	8.16	s	0.1
A-H1′	5.88	d, J(1′,2′) = 4.6	6.33	s	0.45	6.07	d, J(1′,2′) = 3.7	0.19
G-H1′	5.78	d, J(1′,2′) = 4.4	5.90	d, J (1′,2′) = 8	0.12	5.79	s	0
A-H2′	4.68	J(2′,3′) = 4.9	4.37	J(2′,3′) = 4	−0.31			
G-H2′	4.63	J(2′,3′) = 5.2	4.47	J(2′,3′) = 5.5	−0.16			
A-H3′	4.66	J(3′,4′) = 4.7 J(3′,P) = 8.2	4.73	J(3′,4′) = 9.5 J(3′,P) < 0.5	0.07			
G-H3′	4.50	J(3′,4′) = 4.8	4.36	J(3′,4′) = 2	−0.14			
A-H4′	4.32	J(4′,5′) = 2.4	4.45	J(4′,5′) = 3	0.13			
G-H4′	4.31	J(4′,5′) = 2.8 J(4′,P) = 2.2	4.28	J(4′,5′) = 4 J(4′,P) < 0.5	−0.03			
A-H5′	3.82	J(5′,5″) = −12.8	4.26	J(5′,5″) = −13	0.44			
A-H5″	3.79	J(4′,5″) = 3.4	4.11	J(4′,5″) = 2	0.32			
G-H5′	4.30	J(5′,5″) = −11.8 J(5′,P) = 4.0	4.06	J(5′,5″) = −12 J(5′,P) = 4	−0.24			
G-H5″	4.17	J(4′,5″) = 3.6 J(5″,P) = 4.0	3.90	J(4′,5″) = 2 J(5″,P) = 2	−0.27			

[a] Samples 10^{-3} M in D_2O; chemical shifts relative to TSP-d_4. [b] The only assignable signals of the less than 5% abundant isomer are as follows: A-H8, 9.31; G-H8, 8.73; A-H2, 8.32; H1′(s), 6.27; H1′(d), 5.98. [c] Legend: s = singlet; d = doublet. [d] Chemical shift variation relative to ApG.

Table II. T_1 Relaxation Times[a] and Nuclear Overhauser Effects (2D NOESY)[b] for the Characteristic Protons of ApG·*cis*-Pt (**1**)

	A-H8	G-H8	A-H2	G-H1′	A-H1′	A-H3′	G-H2′
T_1, s	0.82	0.82	2.9	2.0	1.8	0.60	0.58
T_1 after H8/D exchange, s			3.0	2.1	1.8	(W)[c]	0.71

[a] At 250 MHz, pH* 6.5, and 17 °C. [b] Correlated NOE's are indicated by the arrows. [c] Not measured because of the water signal.

of ApG and complexes **1** and **6**. The G-H8, A-H8, and A-H2 chemical shifts of complexes **1** and **6**, plotted as a function of pH*,[32] respectively, in the ranges 1–10.5 and 2–9.5 (not shown), reveal two groups with apparent pK_a's of 7.8 and ca. 1.5 for **1** and of 8.1 and 3.3 for **6**. The 7.8 and 8.1 values can be assigned to the NH1 of a N7-platinated guanine (compared to ca. 10.5 in free ApG).[12,33] The 1.5 and 3.3 pK_a's can be respectively attributed to the N1 of a N7-platinated adenine[28,34] and the N1 of an unbound adenine[35] (compared to 3.5 for free ApG). This supports AN7-GN7 platinum chelation of the *cis*-Pt(NH$_3$)$_2^{2+}$ moiety in complex **1** and GN7 coordination of the Pt(dien)$^{2+}$ moiety in complex **6**.

For complexes **1** and **6**, the G-H8 downfield shifts (Table I) are compatible with those reported for G-N7 platination (0.3–0.7 ppm)[12,33,36] and the large A-H8 downfield shift of complex **1** is in agreement with those reported for A-N7 platination (0.6–1.04 ppm).[12a,36] It is noteworthy that A-H1′ of complex **1** and G-H1′ of complex **6** present no coupling constant with their neighboring H2′, revealing an N type (C3′-endo) conformation of the corresponding ribose.[37]

A-H8 and G-H8 of ApG are exchanged in D_2O, at 37 °C and pH 9.6, with respective $t_{1/2}$ values of 7 and 2.5 days. For complex **1** the A-H8 exchange is the fastest with a $t_{1/2}$ value of 20 min at pH* 7 compared to 4 h for G-H8 at pH* 8.8, both at room temperature. An increase of the G-H8 deuterium exchange rate at basic pH* can usually be related to G-N7 platination,[12,33] and

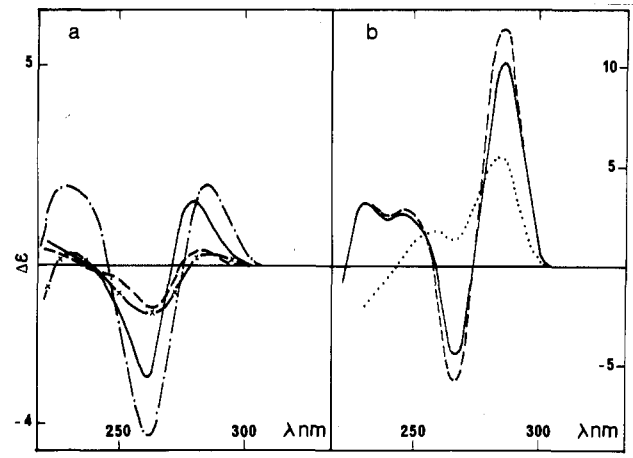

Figure 1. Circular dichroism spectra (in 0.05 M NaCl): (a) ApG, 1.4 × 10^{-4} M, pH 6.8 (—) and 1.9 (- - -), and ApG·Pt(dien) (**6**), 1.4 × 10^{-4} M, pH 7.6 (-·-) and 2.4 (- × -); (b) ApG·*cis*-Pt (**1**), 0.5 × 10^{-4} M, pH 6.5 (—), 2.4 (- - -), and 10.2 (···).

A-N7 platination leads to a fast A-H8 exchange at neutral pH*.[12a,36c]

Table II gives the T_1 relaxation times of the characteristic protons of ApG·*cis*-Pt (**1**) and indicates the protons that present correlated nuclear Overhauser effects (2D NOESY). The relaxation times of the base protons are in agreement with their assignments, particularly the large value for A-H2.[38,39] One can stress three observations: (i) A-H8 and G-H8 present correlated NOE values and the same T_1 value. No effect is detected with their respective H1′ atoms. (ii) G-H8 and G-H2′ present correlated NOE values and the T_1 relaxation time of G-H2′ is increased by 22% after G-H8 deuterium exchange. (iii) Correlated

(32) pH* values are not corrected for D_2O since the pK_a values determined in D_2O, with use of the pH* scale, are practically equal to those determined in H_2O. See footnote 11 in: Scheller-Krattiger, V.; Martin, R. B. *J. Am. Chem. Soc.* **1981**, *103*, 6833–6839.
(33) Chu, G. Y. H.; Mansy, S.; Duncan, R. E.; Tobias, R. S. *J. Am. Chem. Soc.* **1978**, *100*, 593–606.
(34) Inagaki, K.; Kuwayama, M.; Kidani, Y. *J. Inorg. Biochem.* **1982**, *16*, 59–70.
(35) Martin, R. B.; Mariam, Y. H. *Met. Ions Biol. Syst.* **1979**, *8*, 57–124.
(36) (a) Kong, P. C.; Theophanides, T. *Inorg. Chem.* **1974**, *13*, 1167–1170. (b) Kong, P. C.; Theophanides, T. *Bioinorg. Chem.* **1975**, *5*, 51–58. (c) Kong, P. C.; Theophanides, T. *Inorg. Chem.* **1974**, *13*, 1981–1985.
(37) Altona, C. *Recl. Trav. Chim. Pays-Bas* **1982**, *101*, 413–433.
(38) Ts'o, P. O. P.; Barrett, J. C.; Kan, L. S.; Miller, P. S. *Ann. N.Y. Acad. Sci.* **1973**, *222*, 290–306.
(39) Tran-Dinh, S.; Neumann, J. M.; Huynh-Dinh, T.; Igolen, J.; Kan, S. K. *Org. Magn. Reson.* **1982**, *18*, 148–152 and references therein.

Table III. ^{1}H NMR Data for the GpA Complexes: *cis*-[Pt(NH$_3$)$_2$(GpA-*N7*(1),*N1*(2))]$^+$ (**2**) and [Pt(dien)(GpA-*N7*(1))]$^+$ (**7**)[a]

	GpA (pH* 7)		GpA·*cis*-Pt (**2**) (pH* 7.14)			GpA·Pt(dien) (**7**) (pH* 6.03)		
	δ	J, Hz	δ	J, Hz	$\Delta\delta$[b]	δ	J, Hz	$\Delta\delta$[b]
A-H8	8.31	s	8.46	s	0.15	8.36	s	0.05
G-H8	7.87	s	8.34	s	0.47	8.34	s	0.47
A-H2	8.09	s	7.77	s	−0.32	8.26	s	0.17
A-H1′	6.05	d, J(1′,2′) = 4.2	6.04	d, J(1′,2′) = 5.5	−0.01	6.12	d, J(1′,2′) = 3	0.07
G-H1′	5.67	d, J(1′,2′) = 4.0	5.89	s	0.22	5.79	d, J(1′,2′) = 1	0.09

	GpA (pH* 7)		GpA·*cis*-Pt (**2**) (pH* 8, 90 °C)		
	δ	J, Hz	δ	J, Hz	$\Delta\delta$[b]
A-H2′	4.63	J(2′,3′) = 5.4	4.96	J(2′,3′) ≃ 5.5	0.33
G-H2′	4.66	J(2′,3′) = 5.1	≃4.52		−0.14
A-H3′	4.53	J(3′,4′) = 5.3	4.56	J(3′,4′) = 3.5	0.03
G-H3′	4.65	J(3′,4′) = 5.2 J(3′,P) = 8.0	4.21		−0.44
A-H4′	4.39	J(4′,5′) = 2.5 J(4′,P) = 2.0	4.35		−0.04
G-H4′	4.31	J(4′,5′) = 2.7	4.18	J(4′,5′) = 2	−0.13
A-H5′	4.31	J(5′,5″) = −11.8 J(5′,P) = 3.7	≃4.16		−0.15
A-H5″	4.18	J(4′,5″) = 3.0 J(5″,P) = 3.9	4.07		−0.11
G-H5′	3.84	J(5′,5″) = −13	3.94	J(5′,5″) = −13	0.1
G-H5″	3.79	J(4′,5″) = 4	3.81	J(4′,5″) = 4	0.02

[a] Samples 10^{-3} M in D_2O; chemical shifts relative to TSP-d_4. [b] Chemical shift variation relative to GpA.

NOE values exist between A-H8 and A-H3′.

CD spectra at different pHs are presented for ApG and complex **6** in Figure 1a and for ApG·*cis*-Pt (**1**) in Figure 1b. In contrast to the signals of ApG and complex **6**, the large intensity of the signal of complex **1** is not decreased by acidification down to pH 2.4 due to AN7 and GN7 platinum coordination. At basic pH (10.8, 11.1) the signals of ApG and **6** are very little affected (not shown) whereas that of **1** is modified due to G-NH1 deprotonation. These data are comparable with those previously found for the N7,N7 platinum chelates of the GG dinucleotides.[12]

The very minor adduct formed together with ApG·*cis*-Pt (**1**) appears also as a N7,N7 platinum chelate from the chemical shifts of the base protons (Table I, footnote *b*) and the absence of protonation of the N7 sites. The slower A-H8 deuterium exchange compared to that of complex **1** suggests a shielding effect of a polar group due to a "head to tail" structure of the two purines (one syn, one anti).[12a,26,27]

GpA Complexes: *cis*-[Pt(NH$_3$)$_2$(GpA-*N7*(1),*N1*(2))]$^+$ (2) and [Pt(dien)(GpA-*N7*(1))]$^+$ (7). Table III gives the ^{1}H NMR data of GpA and complexes **2** and **7**. The plots of the G-H8, A-H8, and A-H2 chemical shifts of complex **7** vs. pH*, between pH* 2 and 10.5 (not shown), reveal two groups with apparent pK_a's of 8.3 and ca. 3.3. These can be respectively assigned to the NH1 of the N7-platinated guanine[12,33] and to N1 of the unbound adenine[35] (compared respectively to more than 11 and 3.5 in free GpA). This supports G-N7 coordination of the Pt(dien)$^{2+}$ moiety in complex **7**. The same plots for the GpA·*cis*-Pt (**2**) complex are shown in Figure 2. They reveal no protonation down to pH* 1.3, thus excluding the presence of a free G-N7 (pK_a ca. 2.4) or a free A-N1 of either an unplatinated adenine (pK_a 3.5) or a N7-platinated adenine (pK_a 1.2–1.5).[28,34] Moreover, they all present a chemical shift decrease between pH* 6 and 10 with a subdivision into two curves for A-H8 and G-H8 and a line broadening for A-H2. This phenomenon is reversed upon acidification. The chemical shift variation seems to overlap with the titration of a group with an apparent pK_a of ca. 8 (G-H8 plot) that could be assigned to the NH1 of the N7-platinated guanine. From pH* 3 to 6.5, the G-H8, A-H8, and A-H2 signals broaden (from 4 to 14 Hz at half-height for the first two and from 2 to 4 Hz for the third one) before their subdivision at high pH* (Figure 2). This suggests the coexistence of two species that become distinct vs. the NMR time scale at high pH*.

For complexes **2** and **7**, the G-H8 downfield shifts (Table III) are compatible with those reported for G-N7 platination.[12,33,36] For complex **2** the A-H8 and A-H2 chemical shifts do not reflect A-N7 platination[12,36] (compare to **1**, Table I). Moreover, the

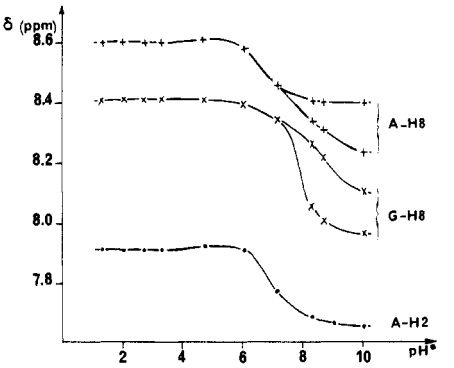

Figure 2. Plots of the chemical shift vs. pH* dependence of the nonexchangeable base protons of GpA·*cis*-Pt (**2**) at 20 °C.

A-H2 signal is shifted upfield whereas N1 platination of AMP leads to a 0.6 ppm downfield shift of this proton.[36b] G-H3′ of complex **2** is also strongly upfield shifted. G-H1′ of complexes **2** and **7** respectively exhibit no and a very small (1 Hz) coupling constant with the neighboring H2′, indicating a predominantly N type conformation of their corresponding ribose.[37]

A-H8 and G-H8 of GpA are exchanged in D_2O, at 37 °C and pH* 9.6, with respective $t_{1/2}$ values of 8 days and 27 h. For complex **2**, at 37 °C and pH 9, the A-H8 exchange is accelerated with a $t_{1/2}$ value of 52 h, whereas that of G-H8 is slowed down with a $t_{1/2}$ value of 20 days. The A-H8 exchange rate in complex **2** indicates that adenine is not bound through its N7 because a much larger acceleration would be expected (vide supra).[12a,36c] Moreover, the large slowing down of the G-H8 exchange suggests shielding effects by neighboring polar groups as already encountered for some CG and GC platinum chelates.[12a,26,27] All these data support GN7-AN1 platinum chelation of the *cis*-Pt(NH$_3$)$_2^{2+}$ moiety in complex **2**.

To get further insight into the two forms of complex **2** detected by ^{1}H NMR, we have studied the influence of temperature on their A-H8, G-H8, and A-H2 chemical shifts at pH* 10.2, for which they have clearly distinct spectra. The curves presented in Figure 3 support the existence of an equilibrium between the two forms distinct at basic pH*, with a coalescence temperature of about 60 °C in these conditions.

At pH* 10.2, before deuterium exchange of the purine H8 protons has occurred, the T_1 relaxation time of A-H2 of complex **2** is 1.2 s (250 MHz, 20 °C). This is relatively short, as compared for example to 2.9 s for A-H2 of ApG·*cis*-Pt (**1**) (Table II). After

Table IV. ^{1}H NMR Data for the GpA Complexes: *cis*-[Pt(NH$_3$)$_2$(GpA-*N*7(1),*N*7(2))]$^+$ (3–5)

	GpA·*cis*-Pt (3) (pH 6.5)			GpA·*cis*-Pt (4) (pH 6.5)			GpA·*cis*-Pt (5) (pH 6.5)		
	δ	J, Hz	$\Delta\delta^b$	δ	J, Hz	$\Delta\delta^b$	δ	J, Hz	$\Delta\delta^b$
A-H8	8.50	s	0.19	9.41	s	1.1	9.15	s	0.84
G-H8	8.50	s	0.2	8.61	s	0.74	8.66	s	0.79
A-H2	8.29	s	0.2	8.35	s	0.26	8.31	s	0.22
A-H1′	5.86	d, J(1′,2′) = 3	−0.2	6.17	d, J(1′,2′) = 8.3	0.12	6.18	d, J(1′,2′) = 5.9	0.13
G-H1′				6.01	s	0.34	6.04	s	0.37
A-H2′				4.82	J(2′,3′) = 5.4	0.19	4.53	*c*	−0.1
G-H2′				4.26	J(2′,3′) = 4.4	−0.4	5.02	J(2′,3′) = 4.4	0.36
A-H3′				4.53	J(3′,4′) = 2	0	4.55	J(3′,4′) = 1.5	0.07
G-H3′				4.92	J(3′,4′) = 9.3	0.27	4.78	J(3′,4′) = 8.5	0.13
					J(3′,P) = 9.3			J(3′,P) = 8.5	
A-H4′				4.42	J(4′,5′) = 2.9	0.03	4.60	J(4′,5′) = 1.5	0.21
					J(4′,P) = 1.5			J(4′,P) = 2	
G-H4′				4.36	J(4′,5′) = 1.9	0.05	4.18	J(4′,5′) = 1.5	−0.13
A-H5′				4.22	J(5′,5″) = −12.2	−0.09	4.35	J(5′,5″) = −12	0.04
					J(5′,P) = 4.4			J(5′,P) = 1.5	
A-H5″				4.03	J(4′,5″) = 1.5	−0.15	4.28	J(4′,5″) = 2.9	0.1
					J(5″,P) = 1.5			J(5″,P) = 4.4	
G-H5′				4.10	J(5′,5″) = −13.2	0.26	3.43	J(5′,5″) = −13.7	−0.41
G-H5″				3.91	J(4′,5″) = 2.9	0.12	3.17	J(4′,5″) = 2.5	−0.62

[a] Samples 10^{-3} M in D_2O; Chemical shifts relative to TSP-d_4. [b] Chemical shift variation relative to GpA. [c] Not determined because A-H2′ and A-H3′ of **5** are nearly isochronous and their signals are superimposed with that of A-H3′ of **4**.

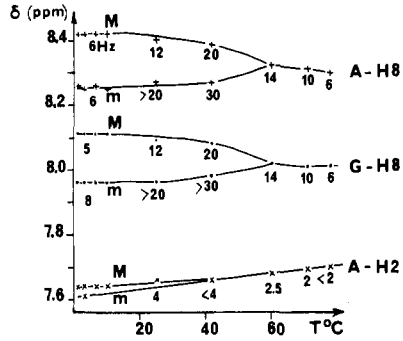

Figure 3. Plots of the chemical shift vs. temperature dependence of the nonexchangeable base protons of GpA·*cis*-Pt (**2**) at pH* 10.2 (see Figure 2). The numbers along the plots indicate the line widths of the signals at half-height. M and m respectively correspond to the signals of the major and minor isomers.

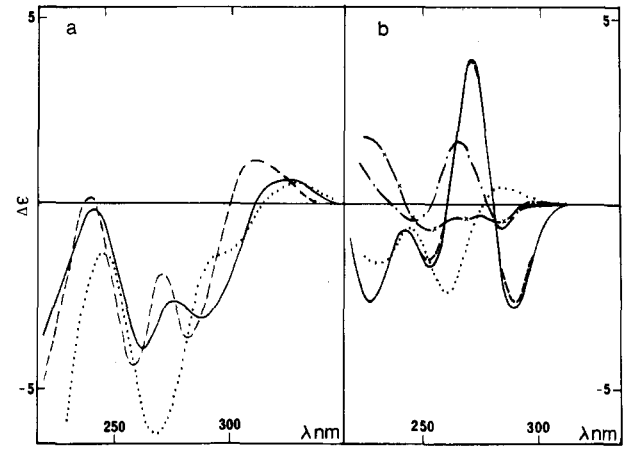

Figure 4. Circular dichroism spectra (in 0.05 M NaCl): (a) GpA·*cis*-Pt (**2**), 1.15×10^{-4} M, pH 7.1 (—), 1.7 (- - -), and 10.8 (···); (b) GpA, 1.3×10^{-4} M, pH 6.8 (– · –), GpA·Pt(dien) (**7**), 1.7×10^{-4} M, pH 6.3 (– × –), and GpA·*cis*-Pt (**3** + **4** + **5**), overall concentration 1.5×10^{-4} M, pH 6.5 (—), 1.9 (- - -), and 10 (···).

the G-H8 to G-D8 exchange, the A-H2 relaxation time is decreased by 30% (0.85 s at 20 °C), thus excluding a major G-H8 contribution to the A-H2 relaxation.[40] Still at pH* 10.2, an increase of temperature from 1 to 42 °C leads to a decrease of the A-H2 T_1, from 1.2 to 0.8 s, and also to small decreases of the A-H1′ and G-H1′ T_1 values (respectively from 0.85 to 0.6 s and 1 to 0.9 s). This is opposite to the normal trend,[41] as observed for example for A-H2 of complex **1** (whose T_1 increases from 2.5 to 3.5 s for the same temperature variation) and for the protons of the complexes **3**–**5** (vide infra, Table V).

These results suggested a chemical environment exchange for the adenine protons of complex **2** due to a conformational equilibrium. Therefore, we have run magnetization transfer experiments, at pH* 10.1 in 80:20 D_2O/CD_3OD, for the well-separated A-H8 signals of the two isomers, respectively, at 8.47 ppm (major one) and 8.33 ppm (minor one). Experiments were run at 18 and −5 °C, respectively, for the slow-exchanging and nonexchanging systems (250 MHz). The use of selective and nonselective inversion recovery in both cases allowed the determination of the rate of exchange between the two conformers at 18 °C.[42] The rate constant for the conversion of the major conformer into the minor one (respectively 65:35 at equilibrium at 18 °C) is $k_1 = 1.4 \pm 0.2$ s^{-1} ($k_{-1} = 2.6 \pm 0.3$ s^{-1}).

Figure 4 presents the CD spectra of GpA·*cis*-Pt (**2**) (Figure 4a) and GpA and complex **7** (Figure 4b). At different pHs, the CD spectra of complex **2** appear composite, a fact that could be related to the coexistence of the two conformers shown by NMR. The signal is largely modified at basic pH. It is noteworthy that the overall signal appears inverted when compared to that of GpA (and also to those of the mixture of the isomers **3**–**5** (Figure 4b) vide infra). The very small intensity of the signal of complex **7** at pH 6.3 is nearly unaffected by acidification to pH 1.9 (not shown).

GpA Complexes: *cis*-[Pt(NH$_3$)$_2$(GpA-*N*7(1),*N*7(2))]$^+$ (3–5). Table IV gives the ^{1}H NMR data for the complexes **3**–**5**, obtained from the study of their mixture in the same HPLC fraction (vide supra).

The plots of the G-H8, A-H8, and A-H2 chemical shifts of GpA·*cis*-Pt (**4**, **5**) vs. pH* between 1.1 and 9.8 (not shown) are parallel for each type of proton and show the same titrations of two groups with apparent pK_a's of 8.2 and 1.3, which can be respectively assigned to the NH1 of a N7-platinated guanine[12,13] and to the N1 of a N7-platinated adenine.[28,34] In the case of complex **3**, the G-H8 and A-H8 plots overlap until the G-NH1 titration occurs (pK_a ca. 8.5), revealing GN7 platination, and the A-H2 plot shows the N1 titration of a N7-platinated adenine (pK_a

(40) Neumann, J. M.; Guschlbauer, W.; Tran-Dinh, S. *Eur. J. Biochem.* **1979**, *100*, 141–148.
(41) Martin, M. L.; Martin, G.; Delpuech, J. J. *Practical NMR Spectroscopy*; Heyden and Sons Ltd.: London, 1980; pp 14–20.
(42) Campbell, I. D.; Dobson, C. M.; Ratcliffe, R. G.; Williams, R. J. P. *J. Magn. Reson.* **1978**, *29*, 397–417.
(43) Marquardt, D. N. *J. Soc. Ind. App. Math.* **1963**, *11*, 431–441.

Table V. T_1 Relaxation Times[a] and Nuclear Overhauser Effects[b] for the Characteristic Protons of the GpA·*cis*-Pt Complexes **3–5**

	GpA·*cis*-Pt (**3**) (pH* 7)				GpA·*cis*-Pt (**4**) (pH* 7)				GpA·*cis*-Pt (**5**) (pH* 7)			
		T_1, s	T_1(D8), s[c]			T_1, s	T_1(D8), s[c]			T_1, s	T_1(D8), s[c]	
	δ	20 °C	20 °C	60 °C	δ	20 °C	20 °C	60 °C	δ	20 °C	20 °C	60 °C
A-H8	8.50	1.05			9.40	0.64			9.16	1.20		
G-H8	8.50	1.05			8.65	0.52			8.69	0.40		
A-H2	8.29	0.95	1	2.2	8.36	2.40	2.50	3.90	8.32	2.30	2.30	3.50
A-H1′	5.86	0.90	1.2	1.55	6.18	1.80	1.80	2.70	6.18	1.80	1.80	2.70
G-H1′					6.02	1.60	1.60	2.50	6.04	1.60	1.60	2.50
A-H2′					4.83	0.6 (W)[d]	(W)[d]	1.80	4.53	0.69	0.73	1.30
G-H2′					4.26	0.53	0.65	0.9	5.02	(W)[d]	(W)[d]	1.20
G-H3′					4.92	0.5 (W)[d]	0.6 (W)[d]	1.1	4.78	(W)[d]	(W)[d]	(W)[d]

[a] At 250 MHz. [b] Correlated NOE's (from 1D or 2D experiments—see text) are indicated by the arrows. [c] T_1 measured after deuterium exchange of A-H8 and G-H8. [d] Less accurately measured or not measured because of the water signal.

ca. 1).[34] This suggests that the three isomers are GN7-AN7 chelates of the *cis*-$Pt(NH_3)_2^{2+}$ moiety.

The G-H8 and A-H8 downfield shifts for the isomers **4** and **5** (Table IV) are compatible with GN7 and AN7 platination.[12,33,36] Those of complex **3** are not characteristic and suggest the superimposition of anisotropy effects. It is noteworthy that G-H2′ of complex **4** is strongly upfield shifted whereas that of the isomer **5** is downfield shifted. Moreover, the reverse trend is observed for G-H5′ and G-H5″. For both complexes **4** and **5**, G-H1′ appears as a singlet, indicating a N type conformation for the ribose.

A-H8 of the isomers **4** and **5** is easily exchanged in D_2O, at pH* 7.4 and 20 °C, with a $t_{1/2}$ of about 15 min in agreement with AN7 platination.[12a,36c] At pH 5.7 and 80 °C, the rate constants for the H/D exchange of A-H8 of the major (**4**) and minor (**5**) complexes are respectively $k = 0.60 \pm 0.06$ and 0.54 ± 0.06 h^{-1}. For the same complexes at pH* 7.7 and 80 °C, the rate constants for the G-H8 exchange are identical: $k = 0.88 \pm 0.09$ h^{-1}. Therefore, within experimental error, the deuterium-exchange rates appear to be the same for the A-H8 and for the G-H8 atoms of both isomers. We could not follow accurately the exchange of the H8 protons of isomer **3**.

Table V gives the T_1 relaxation times of the characteristic protons of the complexes **3–5**, before and after the deuterium exchange of the A-H8 and G-H8 protons. It also indicates the protons that present correlated nuclear Overhauser effects. One can stress the following observations: (i) For complex **3**, the T_1 values of A-H2 and of the only observable H1′ are very short for this type of proton. The T_1 value of H1′ is increased by 33% after H8–deuterium exchange, indicating a H8–H1′ proximity.[40] (ii) For complex **4** A-H8 and G-H8 present a 10% nuclear Overhauser enhancement and have similar T_1 values whereas those values of these protons in complex **5** are very different (with a much longer value for A-H8). (iii) For complex **4**, G-H8 presents NOE's with G-H2′ and G-H3′ and accordingly the T_1 values of these two protons are respectively increased by 22 and 20% in the presence of G-D8.[40] 2D NOESY also reveals a correlation between A-H8 and A-H2′ (that could not be confirmed in 1D because of the water signal). (iv) For complex **5**, the only 2D NOESY correlations observed are between G-H8 and both G-H2′ and G-H3′. No NOE could be detected between A-H8 and the ribose protons. (v) As already mentioned, at variance with the case for complex **2**, the T_1 values of the protons of the isomers **3–5** all increase with temperature in a normal way.[41]

Figure 4b presents the CD spectra of the mixture of the isomers **3–5** at different pHs. The overall signal is of the same type as that of GpA. The influence of the pH is in agreement with N7,N7 platinum binding, with a very small effect of acidification and a large modification due to G-NH1 deprotonation at basic pH.

Kinetics of First Platination and of Metal Chelation for ApG and GpA Reacting with *cis*-$[Pt(NH_3)_2(H_2O)_2](NO_3)_2$. The kinetic studies were done with *cis*-$[Pt(NH_3)_2(H_2O)_2](NO_3)_2$ to avoid superimposition of the aquation reactions of the chloride ligands occurring in the case of *cis*-DDP.[3,44] They were run with 0.1–0.4 mM platinum concentrations, at pH 5.2 and 20 °C, conditions under which the diaqua and aqua hydroxo species are predominant ($pK_{a1} = 5.5$, $pK_{a2} = 7.1$)[3] and do not give significant dimerization.[45]

Table VI. Rate Constants Deduced from the Analysis of the UV Data of the Reaction of ApG with *cis*-$[Pt(NH_3)_2(H_2O)_2](NO_3)_2$[a]

[*cis*-$Pt(H_2O)_2$], mM	$10^4 k_{1,app}$, s^{-1}	k_1, $M^{-1}\cdot s^{-1}$	$10^4 k_2$, s^{-1}	reduced χ^2 for data fit
0.10	1.74	1.74	1.70	2.1×10^{-4}
0.15	2.67	1.78	1.45	1.1×10^{-4}
0.20	3.28	1.64	1.60	4.5×10^{-5}
0.25	3.74	1.50	1.55	2.1×10^{-5}
0.40	7.37	1.84	1.48	3.2×10^{-4}

[a] Conditions: ApG 0.01 mM in water, pH 5.2, 20 °C.

For both ApG and GpA the formation of the platinum chelates involves two steps. The appearance and disappearance of an intermediate complex can be followed by UV, due to a new 280-nm absorption, and by HPLC. The kinetic scheme corresponds to two consecutive steps

$$D + cis\text{-}Pt(H_2O)_2 \xrightarrow{k_1} I \xrightarrow{k_2} C$$

where D = dinucleotide, I = intermediate, and C = chelate(s). Working under pseudo-first-order conditions for step 1 with an excess of *cis*-$[Pt(NH_3)_2(H_2O)_2](NO_3)_2$ gives the simple scheme

$$D \xrightarrow{k_{1,app}} I \xrightarrow{k_2} C$$

for which

$$[D] = [D]_0 e^{-k_{1,app}t}$$

$$[I] = \frac{k_{1,app}[D]_0}{k_{1,app} - k_2}(e^{-k_2 t} - e^{-k_{1,app}t})$$

ApG Case. The analysis (see Experimental Section) of the UV absorbance data recorded for the appearance and disappearance of the intermediate complex gave the $k_{1,app}$ and k_2 values reported in Table VI. From these results one gets $k_1 = 1.7 \pm 0.1$ $M^{-1}\cdot s^{-1}$ (from the slope of $k_{1,app}$ vs. [*cis*-$Pt(H_2O)_2$]) for the first platination step and $k_2 = (1.5 \pm 0.1) \times 10^{-4}$ s^{-1} (mean value ± standard deviation) for the chelation to ApG·*cis*-Pt (**1**). The $k_{1,app}$ values were also checked from the absorbance data relative to the disappearance of ApG. The reaction was also analyzed from the HPLC data (ApG, 1 mM; *cis*-$Pt(H_2O)_2$, 10–15 mM) recorded for the disappearance of ApG and that of the intermediate complex. The same treatment of the data gives $k_1 = 1.6 \pm 0.2$ $M^{-1}\cdot s^{-1}$ and $k_2 = (1.6 \pm 0.3) \times 10^{-4}$ s^{-1} (mean value ± standard deviation) in good agreement with the UV results.

GpA Case. The analysis of the UV absorbance data recorded for the appearance and disappearance of the intermediate complex

(44) Segal, E.; Le Pecq, J. B. *Cancer Res.* **1985**, *45*, 492–498.

(45) (a) Rosenberg, B. *Biochimie* **1978**, *60*, 859–867. (b) Gill, D. S.; Rosenberg, B. *J. Am. Chem. Soc.* **1982**, *104*, 4598–4604. (c) Reference 3.

Table VII. Rate Constants Deduced from the Analysis of the UV Data for the Reaction of GpA with *cis*-$[Pt(NH_3)_2(H_2O)_2](NO_3)_2$[a]

$[cis\text{-}Pt(H_2O)_2]$, mM	$10^4k_{1,app}$, s^{-1}	k_1, $M^{-1}\cdot s^{-1}$	10^4k_2, s^{-1}	reduced $10^3\chi^2$ for data fit
0.10	0.85	0.85	4.50	1.0
0.15	1.20	0.80	3.95	5.0
0.20	1.52	0.76	4.30	1.1
0.25	1.95	0.78	5.10	1.0

[a] Conditions: GpA 0.01 mM in water, pH 5.2, 20 °C.

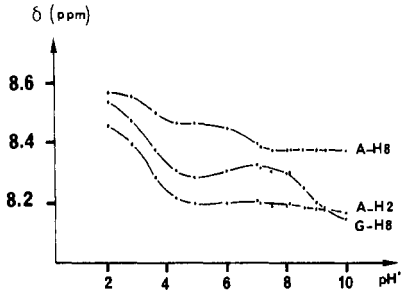

Figure 5. Plots of the chemical shift vs. pH* dependence of the AH8, AH2, and GH8 protons of *cis*-$[Pt(NH_3)_2(H_2O)(ApG\text{-}N7(2))]^+$ (**8**). The AH8 and GH8 assignments were made by using a partially G8 deuteriated ApG (prepared by deuterium exchange in D_2O at basic pH*).

gave the results reported in Table VII. From these, one gets $k_1 = 0.8 \pm 0.1$ $M^{-1}\cdot s^{-1}$ (from the slope of $k_{1,app}$ vs. $[cis\text{-}Pt(H_2O)_2]$) for the first platination step and $k_2 = (4.5 \pm 0.2) \times 10^{-4}$ s^{-1} (mean value ± standard deviation). In this case, k_2 is an overall rate constant for the formation of the four GpA·*cis*-Pt chelates. From the proportions of these isomeric complexes determined by NMR (vide supra), one obtains $k_2(N7,N7) = (3.1 \pm 0.2) \times 10^{-4}$ s^{-1} for the formation of the GpA·*cis*-Pt (**4**, **5**) adducts (N7,N7 chelates anti,anti and anti,syn). The reaction was also analyzed from the HPLC data (GpA, 0.1 mM; *cis*-$Pt(H_2O)_2$, 1–1.5 mM) recorded for the disappearance of GpA and the formation of the GpA·*cis*-Pt (**2**) adduct (N7,N1 chelate). Less accurate HPLC data were also obtained by monitoring the disappearance of the intermediate complex quantified after its trapping by KCl. The same treatment of the data gives $k_1 = 0.7 \pm 0.2$ $M^{-1}\cdot s^{-1}$ and $k_2 = (4.1 \pm 0.2) \times 10^{-4}$ s^{-1} ($k_2(N7,N7) = (2.9 \pm 0.2) \times 10^{-4}$ s^{-1}) (mean value ± standard deviation) in agreement with the UV results.

ApG Intermediate Complex *cis*-$[Pt(NH_3)_2(H_2O)(ApG\text{-}N7(2))]^+$ (8). After 5 min of reaction between ApG (1 mM) and *cis*-$[Pt(NH_3)_2(H_2O)_2]^{2+}$ (10 mM), the intermediate complex **8** represents more than 90% of the mixture containing also ApG and ApG·*cis*-Pt (**1**). This reaction mixture allowed the NMR analysis of the nonexchangeable base protons of complex **8** as a function of pH*. First, **8** was synthesized at pH* 3.6 and the pH* was progressively raised to 9 and decreased to 2 (HNO_3 added). Second, the pH* was raised directly to 10 and progressively decreased to 6.6. The NMR spectra and the HPLC monitoring of the reaction mixture showed the transformation of complex **8** into ApG·*cis*-Pt (**1**) and revealed that it does not occur at a pH* higher than 8.[56] The plots of the AH8, AH2, and GH8 chemical shifts vs. pH* are presented in Figure 5. They reveal three apparent pK_a values at ca. 3.5, 6.5–7, and 8.5. The first and last can be respectively assigned to N1 of an unbound adenine[35] and NH1 of a N7-platinated guanine.[12,33] The second is comparable to the pK_{a2} value of *cis*-$[Pt(NH_3)_2(H_2O)_2]^{2+}$[3] and is assigned to the aqua ligand on platinum. These data show that in complex **8** the *cis*-$Pt(NH_3)_2^{2+}$ moiety is bound to GN7 of ApG and to one aqua ligand.

Discussion

ApG and GpA both react with *cis*-DDP or its diaqua derivative to first give an intermediate complex (vide infra). Whereas in the case of ApG this intermediate gives a single N7,N7 platinum chelate (complex **1**) with less than 5% of another adduct, in the case of GpA four isomeric complexes are formed, one N7,N1 chelate (complex **2**) and three N7,N7 chelates (complexes **3**–**5**).

ApG Complex 1. The AN7,GN7 platinum chelation has been established by monitoring the pH* depdendence of the G-H8, A-H8, and A-H2 NMR signals. It is in agreement with the downfield shifts (Table I) expected from platinum binding and also with the increase of the deuterium-exchange rates of G-H8 and A-H8. T_1 relaxation time and nuclear Overhauser effect data (Table II) show that complex **1** has the anti,anti structure, as revealed by the proximity of the A-H8 and G-H8, G-H8 and G-H2′, A-H8 and A-H3′ protons. The latter points, together with the absence of an A-H1′/A-H2′ coupling constant, show that the 5′- and 3′-riboses respectively adopt N (C3′-endo) and S (C2′-endo) conformations, as already established for the GpG-*cis*-Pt chelate.[12,21] The CD data (Figure 1) agree with the AN7,GN7 anti,anti structure that maintains the overall right-handed helical arrangement of the sugar–phosphate backbone.[26] Therefore, the *cis*-$[Pt(NH_3)_2(ApG\text{-}N7(1),N7(2))]^+$ complex **1** is in every respect comparable to the well-known GpG·*cis*-Pt chelate.

The very minor adduct (less than 5% of the mixture) is also a N7,N7 chelate with a probable "head to tail" arrangement of the purines (see Results).

GpA Complex 2. This complex represents 32% of the mixture of the GpA·*cis*-Pt isomers. The GN7,AN1 platinum chelation is supported by the absence of any protonation of the complex down to pH* 1.3, by the G-H8 downfield shift (Table III), and by the A-H8 deuterium-exchange rate. However, the A-H2 upfield shift and very slow G-H8 deuterium exchange ask for an interpretation. The A-H8, G-H8, and A-H2 chemical shift vs. pH* curves (Figure 2) and the influence of temperature on these chemical shifts at pH* 10.2 (Figure 3) show that complex **2** is composed of two isomers in equilibrium, which become distinct in NMR at basic pH*. At pH* higher than 10, the A-H2 T_1 relaxation data before and after H8–deuterium exchange and at different temperatures suggest a major contribution to the relaxation process of an internal motion of complex **2** whose rate increases with temperature. A magnetization-transfer experiment made with the A-H8 protons of the two interconverting isomers gives a rate constant $k_1 = 1.4 \pm 0.2$ s^{-1} at 18 °C for the transformation of the major into the minor isomer ($k_{-1} = 2.6 \pm 0.3$ s^{-1}). These results can be interpreted by a rotation of the adenine about its glycosidic and N1–Pt bonds. Inspection of space-filling (CPK) and framework (Nicholson) models show that this rotation can cover 180° between one conformer with G-O6 and A-NH_2 in close proximity on the same side of the platinum coordination plane and the other conformer with G-O6 and A-NH_2 on each side of this plane. This rotation involves a gear-wheel-like interaction between A-NH_2 and one ammine ligand on platinum. There is an analogy between this rotation and that already established for the N3-coordinated cytosine of the CpG·*cis*-Pt chelate, the latter being 4 orders of magnitude slower (1.8 (3) $\times 10^{-4}$ s^{-1} at 18.5 °C).[26] The NMR detection of the two conformers of complex **2** at basic pH* appears related to the NH1 deprotonation of the coordinated guanine leading to a slowing down of the adenine rotation. Inspection of the molecular models suggests that this could result from a binding interaction between the 6-carbonyl of the deprotonated guanine and the 6-amino group of the adenine.

The adenine rotation precludes a conclusive assignment of the guanine configuration, based on T_1 relaxation times and nuclear Overhauser effects. The 0.22 ppm G-H1′ downfield shift relative to the signal for GpA (Table III) falls in the 0.15–0.25 ppm range usually found for the G_{syn} GpX·*cis*-Pt chelates compared to 0.3–0.4 ppm found for the G_{anti} isomers (see GpG·*cis*-Pt,[12] GpA·*cis*-Pt (**4** and **5**) (vide infra), and G_{anti} and G_{syn} GpC·*cis*-Pt[27,46]). This suggests a tentative G_{syn} assignment. The guanosine ribose is C3′-endo ($J(H1',H2') = 0$; Table III) as observed for the 5′-ribose of all the described dinucleotide platinum chelates.[12,21,26,27,46] The GN7,AN1 structure of complex **2** with the adenine rotation can explain (i) the A-H2 upfield shift due to its movement in the

(46) Girault, J.-P.; Chottard, G.; Guittet, E. R.; Herman, F.; Chottard, J.-C., to be submitted for publication.

shielding cone of the five-membered ring of the guanine, (ii) the G-H3′ upfield shift (Table III) due to the C3′-endo conformation of the guanosine that puts this proton in the shielding cone of the adenine ring, (iii) the very slow G-H8 deuterium exchange due to its shielding by the NH_2 of the flipping adenine (a phenomenon encountered also in the CpG[26] and GpC series[27,46]), and (iv) the A-H2 relaxation data due to its fluctuating proximity with the G-H8, -H3′, and -H2′ protons.

The CD spectra of complex **2** at various pHs (Figure 4a) can be interpreted as the superimposition of the spectra of the two main rotamers in different proportions and also with different ellipticities at basic pH related to the G-NH1 deprotonation. The overall signal is inverted when compared to that of GpA and of the mixture of the other GpA·*cis*-Pt isomers (Figure 4b). Inspection of the molecular models shows that this inversion can be related to the strong perturbation of the sugar–phosphate backbone imposed by the A-N1 coordination, leading to a left-handed pseudohelical arrangement, as already encountered for the C_{anti},G_{anti} CpG·*cis*-Pt chelate.[26]

GpA Complexes 3–5. These complexes respectively represent 5, 42, and 21% of the mixture of the GpA·*cis*-Pt isomers. The GN7,AN7 platinum chelation for the three isomers has been established by monitoring the pH* dependence of the G-H8, A-H8, and A-H2 chemical shifts. For complexes **4** and **5** the chelation is in agreement with the expected downfield shifts (Table IV) and increase of H8–deuterium exchange rate, due to platinum binding. T_1 relaxation time and nuclear Overhauser effect data (Table V) allow the assignment of the structures of complexes **4** and **5**. Complex **4** is anti,anti, as revealed by the proximity of the G-H8 and A-H8, G-H8, G-H2′, and G-H3′, and A-H8 and A-H2′ protons. Complex **5** is G_{anti},A_{syn} as suggested by the proximity of the G-H8 and G-H2′ and G-H3′ protons and by the absence of any detectable NOE between A-H8 and other protons. Inspection of the molecular models shows that in complex **5** the adenine is actually at the limit of the syn or anti assignment with a χ value (χ = O(4′)C(1′)N(9)C(4))[47] that might be larger than 90° in agreement with the absence of A-H8/A-H1′ NOE. These structures of complexes **4** and **5** can explain (i) the G-H2′ upfield shift in complex **4** due to the ring current effect of the anti A, whereas a downfield shift is observed in **5** with syn A and (ii) the large upfield shifts of G-H5′ and G-H5″ in complex **5** due to the ring current effect of syn A. It is noteworthy that the deuterium-exchange rates of the G-H8 and of the A-H8 protons of both the **4** and **5** complexes, at 80 °C, are identical. Smaller rates would be expected for complex **5** because of the shielding effects of the carbonyl and amino groups on the H-8 of the other base (see GpA·*cis*-Pt (**2**) and the cases of the CpG[26] and GpC[27,46] platinum chelates). The identity of the H8–D exchange rates could result from the existence of a conformational equilibrium between **4** and **5** that might be due to a rotation of the adenine about its N7–Pt and glycosidic bonds. Such an equilibrium could not be investigated because the **4** and **5** isomers were not separable by HPLC. Moreover, between 5 and 80 °C one could not detect any significant variation of the **4** and **5** proportions by NMR.

The third and minor GN7,AN7 chelate, complex **3**, must have a G_{syn} configuration. The T_1 relaxation time data (Table V), clearly show a H8–H1′ proximity, for the only observable H1′, indicative of a syn configuration. The fast relaxation of A-H2 suggests an "internal" situation for this proton and therefore a tentative A_{syn} configuration. Inspection of the CPK molecular models for this G_{syn},A_{syn} structure leads us to assign the only observed H1′ signal to A-H1′ because of its proximity to A-H8. (This is not the case for G-H1′ and G-H8.) This is in agreement with the H1′–H2′ coupling (Table IV), showing that the corresponding ribose has not adopted the C3′-endo conformation characteristic of the 5′-ribose of the dinucleotide platinum chelates.[12,21,26,27,46]

The CD spectra for the **3–5** mixture (Figure 4b) agree with N7,N7 chelation. Compared to the spectrum of free GpA they suggest that complexes **4** and **5** retain an overall right-handed helical arrangement of the sugar–phosphate backbone[26] similar to that of ApG·*cis*-Pt (**1**).

Kinetics of First Platination and Chelation with *cis*-[Pt$(NH_3)_2(H_2O)_2$]$(NO_3)_2$. Kinetic preference for platinum binding to guanine compared to other bases is well-documented.[26,48-50] For ApG the NMR analysis clearly shows that, in the aqua intermediate complex **8**, platinum is bound to GN7. For both ApG and GpA reacting with [PtCl(dien)]Cl, only the GN7-bound complexes **6** and **7** are formed, in agreement with very recent results obtained with d(GpApG).[51] Therefore, the first platination step occurs on GN7. The k_1 rate constants for the first platination of ApG and GpA, respectively 1.7 (1) and 0.8 (1) $M^{-1}\cdot s^{-1}$, reveal a factor of 2 in favor of ApG. The same factor of 2 between the 3′- and 5′-G is found from the ratio of the adducts formed by reaction of [PtCl(dien)]Cl with GpG[52] and d(GpApG).[51] Enhancement of the GN7 platination rate by the presence of a 5′-terminal phosphate has already been observed with 5′-GMP,[49,50,53] d(pGpG),[12b] and d(pGpGpG).[54] Therefore, a similar effect is present with a 5′-connected phosphodiester group but of much less amplitude, with a factor of 2 to be compared to that of about 15 reported between the platinations of 5′-GMP and G.[50] This effect suggests that charge interaction and/or hydrogen bonding occur between the cationic aquated platinum species and the monoanionic phosphodiester group that favor N7 platination on the 3′-base.

The k_2 rate constants, 1.5 (1) × 10^{-4} s^{-1} for the chelation step of the ApG intermediate complex **8** (into ApG·*cis*-Pt (**1**)) and 4.5 (2) × 10^{-4} s^{-1} for the chelation step of the GpA intermediate complex (into the N7,N1 (**2**) and three N7,N7 (**3–5**) GpA·*cis*-Pt complexes), show that complex **8** is a more stable intermediate. It suggests that the 5′-phosphate–platinum complex interaction, mentioned above, is still present in the ApG intermediate complex **8**. Such an interaction is not possible in the GpA intermediate complex. A comparative study of these complexes is in progress. At present, a comparison of the [Pt(dien)(ApG-*N7*(2))]$^+$ (**6**) and [Pt(dien)(GpA-*N7*(1))]$^+$ (**7**) complexes supports this hypothesis. The CD spectra of complexes **6** and **7** compared to those of their parent dinucleotides show a significant increase of the biphasic signal in the case of **6** (Figure 1a) and a large decrease in the case of **7** (Figure 4b). This suggests respectively the presence and absence of a stacking interaction between the purines of complexes **6** and **7**, in agreement with the effect of acidification. The CD data relative to the [Pt$(NH_3)_3$(ApG-*N7*(2))]$^+$ complex, more comparable to those of complex **8**, are in every respect identical with those of complex **6** (to be published). Inspection of the CPK molecular models suggests that a hydrogen bond between a dien amino group and the ApG phosphate would favor a stacking of the purines within the ApG·Pt(dien) complex **6**. Therefore, hydrogen bonding between the phosphate group and a platinum ligand, which should be stronger with H_2O than with NH_3, could explain the slower chelation reaction of the *cis*-[Pt$(NH_3)_2$-(H_2O)(ApG-*N7*(2))]$^+$ intermediate **8** compared to that of the GpA intermediate complex. The existence of an aqua bridge between platinum and the adjacent O6 of the guanine, as proposed from the X-ray study of a platinated dodecamer,[55] does not seem

(47) Davies, D. B. *Prog. Nucl. Magn. Reson. Spectrosc.* **1978**, *12*, 135–225 (Part 3).

(48) Mansy, S.; Chu, G. Y. H.; Duncan, R. E.; Tobias, R. S. *J. Am. Chem. Soc.* **1978**, *100*, 607–616.

(49) Reedijk, J.; den Hartog, J. H. J.; Fichtinger-Schepman, A. M. J.; Marcelis, A. T. M. In *Platinum Coordination Complexes in Cancer Chemotherapy*; Hacker, M. P., Douple, E. B., Krakoff, I. H., Eds.; Martinus Nijhoff: The Hague, The Netherlands, 1984; pp 39–50.

(50) Eapen, S.; Green, M.; Ismail, I. M. *J. Inorg. Biochem.* **1985**, *24*, 233–237.

(51) Van der Veer, J. L.; van der Elst, H.; den Hartog, J. H. J.; Fichtinger-Schepman, A. M. J.; Reedijk, J., personal communication.

(52) The two Pt(dien)(GpG) N7(1) and N7(2) isomers have been isolated by HPLC, characterized by their chemical shift vs. pH profiles, and easily identified by GH8-GH2′ NOE (to be submitted for publication).

(53) Marcelis, A. T. M.; Erkelens, C.; Reedijk, J. *Inorg. Chim. Acta* **1984**, *91*, 129–135.

(54) Reedijk, J.; et al., personal communication.

(55) Wing, R. M.; Pjura, P.; Drew, H. R.; Dickerson, R. E. *EMBO J.* **1984**, *3*, 1201–1206.

to explain our kinetic and CD data.

Conclusions about the Comparison of ApG and GpA. From the comparison of the platinum-binding reactions one can draw the following conclusions: (i) ApG and GpA reacting with *cis*-$[Pt(NH_3)_2(H_2O)_2]^{2+}$ first give GN7 platination to an intermediate complex, followed by a chelation step. (ii) For the first platination step, ApG reacts 2 times faster than GpA due to the influence of the phosphodiester group. (iii) The chelation step of the ApG intermediate complex **8** is 3 times slower than that of the GpA intermediate. This can be attributed to a stabilizing hydrogen bond between a ligand of the GN7-bound cationic platinum species and the anionic phosphodiester group. (iv) This interaction in complex **8** precludes guanine rotation about the glycosidic bond and favors the stacking of the bases, leading practically to the single AN7,GN7 anti,anti ApG·*cis*-Pt chelate **1**. (v) There is no interaction within the GpA intermediate complex to limit the conformational freedom of the bases. Therefore, adenine chelation can occur through the N1 and N7 binding sites, with anti and syn conformations of the bases, leading to one GN7,AN1 (**2**) and three GN7,AN7 (**3–5**) GpA·*cis*-Pt isomeric chelates. (vi) Several of the platinum chelations observed with GpA are not relevant to the case of DNA platination, especially the GN7,AN1 one. But our dinucleotide results show that there is no intrinsic property of the ApG or GpA sequence to explain the absence of d(GpA) adduct in platinated DNA. It is noteworthy that for d(GpApG), even at 80 °C, no GpA chelate is found and the G5′ intermediate complex is only chelated by 3′-GN7.[51] However, this seems mainly due to the greater reactivity of G vs. that of A[50] because, at 80 °C, the conformational mobility of the trinucleotide should enable the adenine binding sites to reach the platinum linked to 5′-GN7 (see GpA), as does the more remote 3′-GN7. Therefore, in the case of a stacked B-DNA type structure, if the first platinated G belongs to a AG or GA sequence, the formation of d(ApG) but no d(GpA) chelate is likely to result from the smaller distance between the platinum and N7 of 5′-A (≃3 Å) than between platinum and N7 of 3′-A (≃5 Å), as previously proposed by Dewan.[11] Within the GN7-coordinated intermediate complex, hydrogen bonding between the 5′-phosphodiester bridge and an ammine or aqua ligand, suggested by our ApG results, should increase the proximity, favoring the chelation by the 5′-neighboring base.

(56) We have checked that complex **8** is unchanged under the HPLC conditions (10^{-2} M $CH_3CO_2NH_4$, pH 4.7) by comparing its retention time with that of the corresponding acetato intermediate prepared by treatment of **8** with 0.2 M $CH_3CO_2NH_4$. HPLC elution with 10^{-2} M NH_4NO_3, pH 4.7, was also used.

Acknowledgments. Support of this work by a grant from the "Association pour la Recherche sur le Cancer" is gratefully acknowledged. We thank Drs. J. Y. Lallemand and E. Guittet for the 400-MHz ^1H NMR spectra and fruitful discussions and Dr. Gouyette for the atomic absorption determinations. Stimulating discussions with the group of Prof. Dr. J. Reedijk were made possible thanks to the sponsorship of the French-Dutch cultural agreement and the Direction de la Coopération et des Relations Internationales. We thank Engelhardt Industries, France, for a loan of platinum salt.

Contribution from the Dipartimento di Scienze Chimiche, Università di Catania, 95125 Catania, Italy, and Department of Chemistry, Brigham Young University, Provo, Utah 84602

Coordination Properties of Cyclopeptides. Formation, Stability, and Structure of Proton and Copper(II) Complexes of *cyclo*-(L-Histidyl-L-histidyl) in Aqueous Solution

Giuseppe Arena,*[1a] Raffaele P. Bonomo,[1a] Giuseppe Impellizzeri,[1a] Reed M. Izatt,*[1b] John D. Lamb,[1b] and Enrico Rizzarelli*[1a]

Received May 23, 1986

Cyclic dipeptides with amino acid residues containing complexing side-chain groups can coordinate to metal ions in a way that mimics the coordination sites in enzymes. In order to obtain an improved understanding of the complexing properties of cyclopeptides involved in biological systems, the interactions in aqueous solution of protons and copper(II) with *cyclo*-(L-histidyl-L-histidyl) (Cyhis) were studied by potentiometric pH titrations and by calorimetry. Values of $\Delta H°$ and $\Delta S°$ for proton interaction with Cyhis suggest that solvophobic forces are involved in the stabilization of the Cyhis folded conformation. Comparison between the enthalpy and entropy changes associated with Cu–Cyhis interaction and those associated with the interaction of Cu^{2+} with imidazole (Im) helps to identify the donor atoms involved in the coordination. The EPR data, namely the superhyperfine pattern arising from the interaction of the odd electron with the nitrogen atoms, confirm the suggestions advanced on the basis of thermodynamic values involving the formation of chelates of unusual ring size for both $[Cu(Cyhis)]^{2+}$ and $[Cu(Cyhis)_2]^{2+}$. In addition, the EPR spectra support the coordination of both nitrogens of the Im residues in the Cu(Cyhis) species. Solvophobic forces have been invoked to explain the thermodynamic values associated with $[Cu_2(Cyhis)_2H_{-2}]^{2+}$ complex formation.

Introduction

Naturally occurring and synthetic cyclic peptides have been the subject of intensive study in recent years[2-6] in modeling protein conformation, membrane transport, and other biological processes associated with ion binding.[7-10] The advantages of these model ligands over linear peptides are their "constrained" geometry and the absence in them of free $-COO^-$ and $-NH_2$ terminal groups. Unlike the case for linear peptides, the deprotonation of the peptide nitrogen occurs in the presence of transition-metal ions at high pH values[11] and therefore, under normal conditions, the macrocyclic peptides coordinate via oxygen atoms only.

Cyclic peptides with amino acid residues containing complexing side-chain substituents such as imidazole (Im), carboxylate, or thioether groups can coordinate to metal ions in a way that mimics the coordination sites in enzymes.[12] In addition, such chains can "encourage" the coordination of peptide nitrogens.[13] Recent studies involving cyclic peptides have focused on the synthesis of their metal complexes and the subsequent characterization of these

(1) (a) Università di Catania. (b) Brigham Young University.
(2) Ovchinnikov, Yu. A.; Ivanov, V. T. *Tetrahedron* **1975**, *31*, 2177.
(3) Deber, D. M.; Madison, V.; Blout, E. R. *Acc. Chem. Res.* **1976**, *9*, 106.
(4) Kessler, H. *Angew. Chem., Int. Ed. Engl.* **1982**, *21*, 512.
(5) Kopple, K. *J. Pharm. Sci.* **1972**, *61*, 1345.
(6) Madison, V.; Atreyl, M.; Deber, C. M.; Blout, E. R. *J. Am. Chem. Soc.* **1974**, *96*, 6725.
(7) Blout, E. R.; Deber, C. M.; Pease, L. G. In *Peptides, Polypeptides and Proteins*; Blout, E. R., Bovey, F. A., Goodman, M., Lotan, N., Eds.; Wiley: New York, 1974; p 266.
(8) Sarkar, B. In *Metal Ligand Interaction in Organic Chemistry and Biochemistry*; Pullman, B., Boldblun, N., Eds.; Reidel: New York, 1977; Part 1, p 193.
(9) Baron, D.; Pease, L. G.; Blout, E. R. *J. Am. Chem. Soc.* **1977**, *99*, 8299.
(10) Pease, L. G.; Watson, C. J. *J. Am. Chem. Soc.* **1978**, *100*, 1279.
(11) Rybka, J. S.; Margerum, D. W. *Inorg. Chem.* **1980**, *19*, 2784.
(12) Isied, S. S.; Kuehn, C. G.; Lyon, J. M.; Merrifield, R. B. *J. Am. Chem. Soc.* **1982**, *104*, 2632.
(13) Brubaker, G. R.; Sakkab, N. Y. *Bioinorg. Chem.* **1974**, *3*, 243.

0020-1669/87/1326-0795$01.50/0